

L.N. López de Lacalle · A. Lamikiz · J. Muñoa · M.A. Salgado · J.A. Sánchez

Improving the high-speed finishing of forming tools for advanced high-strength steels (AHSS)

Received: 22 September 2004 / Accepted: 1 December 2004 / Published online: 28 September 2005
© Springer-Verlag London Limited 2005

Abstract Forming tools manufacturers have extensively incorporated high-speed milling technology for the finishing of large punch or die tools. The main objective is to achieve a good surface quality directly from machining, without any additional, tedious, manual work. Currently, new advanced high-strength steels (AHSS) are being used for car body parts. In this case, there are two special changes related to the forming tools: a higher proportion of harder surfaces on the working area, and long try-out iterations, due to their great springback. Tempered surfaces and insert blocks harder than 60 HRC are needed to withstand the forming charges with a good working life expectancy. From this, two problems arise with regards to high-speed finishing: first, the deflection of the tool due to the cutting forces, which can produce unacceptable dimensional errors; and second, in the same finishing operation, zones with sharp changes in hardness must be machined with the same CNC program and cutting tool.

The key to solving both problems will be the use of newly developed utilities in the preparation stage, and the elaboration of CNC programs using CAM software. In the first case, the deflection of tool is dealt with by a milling model which obtains the values of cutting forces. This model characterises the couple tool/material with six coefficients, which are previously obtained for ball-end milling tools and base die materials. Inputs provided by the CAM user include feed per tooth, and radial and axial depths of cut. The problem of surfaces with areas of different hardness and poorly defined boundaries is solved with a special postprocessor coded in C language. Once the CAM user has defined (on the CAD model) the theoretical boundaries of the tempered areas, the insert blocks or the deposition material areas, this utility includes changes of the programmed feed function in the CNC program.

In this paper, these approaches are applied to medium size workpieces with the same features of the actual punch and die for AHSS forming. Results are provided to die manufacturers for application in real forming tools. This technological model of the milling process estimates values of cutting forces and offers manufacturers a reduction of production and lead times.

Keywords High speed milling · Dies · Moulds · Cutting forces

1 Introduction

Since the late 1990s, great efforts have focused on the reduction of production wastes and the reduction of environmental impacts due to transport [1, 2]. For this, a reduction of the weight of vehicles, and therefore the oil consumption, is a common aim. The automobile industry has introduced and increased the use of new materials such as magnesium (AZ91), high boron steels, austenitic stainless steels and structural aluminium alloys [3]. Steel production companies have researched and developed new products with improved features like high ultimate strengths and yield points. In this way, an answer to the introduction of non-ferrous materials is given. The use of high-strength steel in car bodywork has spread in recent years. The AISI institute is forecasting a dramatic increase in the use of advanced high-strength steels (AHSS) in the automotive industry. The main advantage of these types of steel is a higher impact resistance, which allows for a reduction in the weight of the bodywork components. The new qualities of steels include: high-strength steels (HSS) with yield strengths of 210–550 MPa, ultra high-strength steels (UHSS) with yield strengths greater than 550 MPa, and advanced high-strength steels (AHSS), which can be defined as multi-phase steels. The AHSS group includes transformation induced plasticity steels (TRIP), dual phase steels (DP), and complex phase steels (CP). Compared to HSS and UHSS, AHSS exhibits a superior combination of high-strength and good formability due to their elevated strain hardening capacity (as a result of a lower yield strength/ultimate tensile strength ratio). There is not a common standard for them yet, in view of its novelty. The

L.N. López de Lacalle (✉) · A. Lamikiz · J. Muñoa · M.A. Salgado · J.A. Sánchez
Department of Mechanical Engineering,
University of the Basque Country,
ETSII, c/Alameda de Urquijo s/n, 48013 Bilbao, Spain
E-mail: implomal@bi.ehu.es
Tel.: +34-94-6014216
Fax: +34-94-6014215

yield point/ultimate strength of these steels is around 280/600 MPa for DP280, 700/1000 MPa for DP700, and 350/800 MPa for TRIP 350. Therefore, a stronger action must be applied to deform AHSS metal sheets to a final shape, and there is a high risk of springback. As bending and stamping forces increase, so does the wear of stamping and bending dies.

With regards to reducing wear, a larger number of hardened surfaces are needed where AHSS sheets are to be cut or deformed. These areas can be made of inserts in tempered steel or constructed via the direct tempering of cast iron surfaces (by laser or induction). In the processing of common steels, dies are made on lamellar cast irons, such as GG25, or of steel St52 with few tempered surfaces. Currently, however, the globular iron cast type GGG70 and AISI 1.2379 steels are most widely used, and are hardened with tempering up to 64 HRC.

Therefore, the finishing of dies has gone from the high-speed milling of 220–290 HBN to the high-speed machining of 64 HRC surfaces. An example of a punching tool for a rear bottom part made on AISI 1.237, hardened at more than 64 HRC, is shown in Fig. 1.

There are two problems directly related to the presence of a large number of hard surfaces, in addition to problems of the high speed milling of dies, described in detail in [4, 5]:

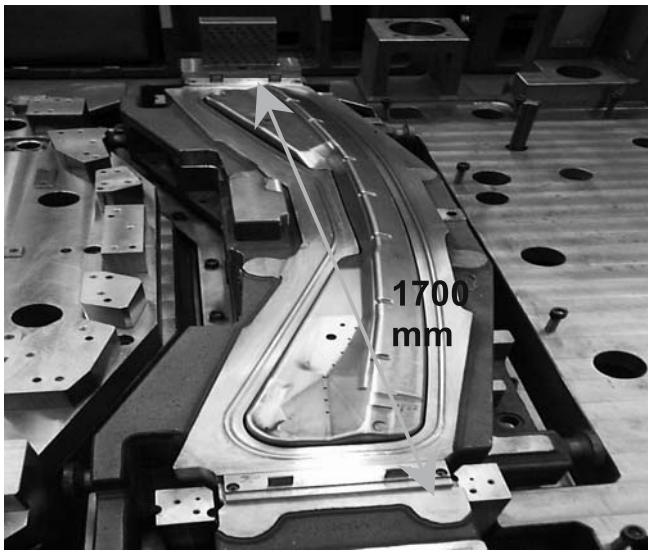
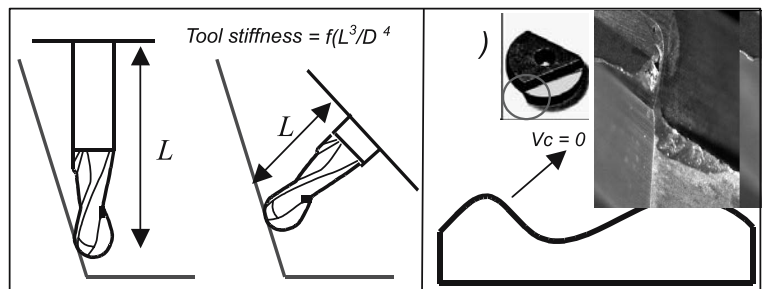


Fig. 1. Punching tool made of tempered steel AISI 1.237, hardened to more than 64 HRC

Fig. 2. Advantages of the five-axes machining of complex surfaces: left – use of tools with less overhang; right – where tool tip cutting speed is zero. Detail of a PCBN breakage located at the tool tip due to low cutting speed



- Dimensional errors in surface result from the deflection of cutting tools. There are important errors associated with the deflection of cutting tools (or the deformation of the entire machine under the action of the cutting force), which are considered in this paper. Tool deflection implies that material is left on the surface, which in some cases can be more than a hundredth of a millimetre. This makes it necessary to repeat the finishing CNC programs, and as such material overstock is eliminated in a second pass. But CNC programs for large dies usually require 20–30 h. The result is wasted time and money, and an increase in lead time in a highly competitive industrial sector [6].
- Large dies with several areas hardened to different levels must be finished by high-speed milling, using the same CNC program and the same milling tool (or set of milling tools). The transition of the tool between surfaces of different hardness can produce tool breakage and marks on surfaces, resulting in a dramatic decrease in process reliability. Transitions between hardened/soft areas are sudden in the case of inserted blocks, or with a poorly defined boundary in the case of areas with a direct tempering of the cast iron surfaces.

AHSS presents a high springback effect, and despite some research, there is not yet adequate simulation software for progressive die developing [7, 8]. Therefore, the tryout stage involves a large number of loops (with respect to the equally long tryout in mild steels forming), and a continuous definition of the punch or die surfaces. Sometimes, changes in this stage lead to the re-machining of the surface. Multiplying this longer stage by the increased time of each finishing results in more time being added to the production of one die set. In short, the production times for an AHSS die is perhaps double that of a forming tool for mild steels.

Common machines in die manufacturing include large gantry milling machines with two- and five- axes spindle heads. The latter offers the possibility of continuous interpolation of five-axes at the same time, typically used in 3 + 2-axes operations. This implies a two-axes orientation of the tool with respect to the machining surface, and a three-axes operation with the rotational axes of the spindle head locked.

Five-axes machines allow the use of shorter, stiffer tools, as shown in Fig. 2(left) [9, 10]. In the same way, a correct orientation of the tool with respect to the surface can avoid milling

with the tip of the ball-end milling tool, where the cutting speed is zero, as shown in Fig. 2 (right). At this point, flaking (heavy chipping) of both tool edges occurs; in [4] some results of a polycrystalline cubic boron nitride (PCBN) tool are presented. In that work, all the machining tests incorporating a PCBN tool showed tool chipping at the tool tip due to the low cutting speed at this point (see detail in Fig. 2). Therefore, five-axes machining is the key for using these expensive but powerful cutting tools; this technique ensures milling without the tool tip cutting, and allows for the changing of the orientation between tool-axis and surface continuously.

The use of high-speed machining to achieve good surface finishing of dies was studied by López de Lacalle et al. [11]. Here, a systematic description of the main industrial problems were given, and a major step towards a stable and optimum industrial application of this technique was made. The use of PCBN was also discussed. This paper extends the López de Lacalle et al. study to include those dies specially designed for the forming of new AHSS steels. We aim to address the following production standards:

- Dimensional error must be less than $50\ \mu\text{m}$. This is an arbitrary mean value of some companies known by the authors. Dimensional tolerances in die manufacturing are not as narrow as in the case of moulds.
- Super-finishing of the die surfaces must be performed after the thermal treatment of some zones of the surfaces, or after the deposition of metal, to solve machining errors. Thermal treatment results in the distortion of surfaces, and if tempering is done after high-speed finishing, a lot of manual polishing work must be done. Thus, if high-speed finishing is applied to a partially hardened surface, it results in big savings in terms of both of time and money.

These objectives will be solved in the computer-aided manufacturing (CAM) planning process stage. This stage is very important in the manufacturing of dies and moulds [9]. In five-axes milling, CAM is at the core of the planning process. As a result, CAM operators play a significant part in the success of the machining operations, because workshop workers can only use machine dials (which modify the actual feed and spindle rotation speed respect to that programmed in the NC code) to change the actual values of cutting speed and feed rate making, and as a result, it is impossible to change tool path directly in the CNC interface. In die manufacturing, the right selection cutting speed and other cutting conditions is important in achieving production efficiency, but is not as critical as in the production of large batches, where the adjustment of these values can significantly change the value of productivity and the final cost per piece [12]. In die manufacturing where parts are unique, process reliability is more important.

In this work, we detail some examples of applications on test parts using a newly proposed programming methodology. The first example is a smooth surface, which is machined at high-speed using a typical three-axes operation and applying three milling strategies; the second example involves a test part with very complex geometry, which is hardened to 64 HRC; and the

third example is a cast iron test part with two hard insert blocks (64 HRC), several tempering zones and metal deposition in a U slot. From our study, it can be seen that recent modelling research efforts can be used to increase the quality, reliability and time savings in industrial applications, thus attaining the fundamental objectives for technological upgrading suggested by technical roadmapping reports [1, 2] and investigations [5].

2 Research methodology: test parts

One problem in research looking to improve the die finishing is the large size of parts and the long time required for each machining operation. Due to these reasons, the application of a systematic approach in real parts is very difficult, unless direct field studies are conducted industrial processes. One solution to drawback is the use of test parts. Several works have achieved successful results with test parts [13–17] in complex surface machining problems. This approach allows researchers to carry out successive laboratory machining tests with reduced times and costs. Test parts must include the same main features, base material and treatment, and geometry (slopes, fillet radii, depth) of real parts to allow for the extrapolation of research conclusions to real production. In this research, three test parts were designed by die manufacturers. All of them are $260 \times 260\ \text{mm}$ in size, and the same than the dynamometer plate (Kistler 9255B) was used in tests. Thus, tests could be performed to collect the cutting force during machining. In the next subsection, test parts are briefly described.

2.1 Complex surface test part (CSP)

The CSP part is made of AISI H13 hardened steel, a chromium-molybdenum-vanadium alloyed steel, 54 HRC, with four similar smooth freeform surfaces without any sharp edge inside of them. The geometry of this part is similar to ceilings, bonnets and other large surfaces, although the material is harder than the cast irons commonly used in the construction of these parts. In this case, the main aim of research is the selection of the best machining direction.

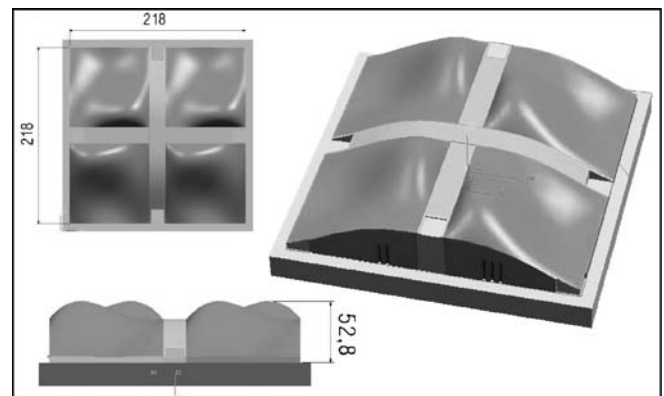


Fig. 3. CSP test part

2.2 High hardness test part (HHP)

The HHP part is made of DIN 1.2379 (AISI type D3) steel tempered at 64 HRC. This is a high-carbon (1.4%–1.6%), high-chromium (11%–13%) tool steel, and is virtually non-deforming during heat treatment. The geometry of the part shows some special features which are common in different insert blocks of dies and punches. Our objective here is not to make one correct piece, but to gain knowledge about all the cases present in the test part, including:

- The maximum depth is 110 mm and the fillet radius is 4.5 mm, which suggests the use of long and slender tools with diameters of 16 mm and lengths of more than 25 mm.

Other tools are less than 6 mm in diameter, and in this case, use thermal shrinkage tapered toolholders.

- Inclined surfaces from 0 to near 90°, the usual values of slope in cutting punches.
- Several nerves and slots.

Figure 4 shows the test piece and some details of its complex geometry.

For this test part, our main goals were to assess the selection of good (near-optimal) tool orientation with respect to the normal to the surface to be machined (tilt angle, α), and the angle of the feed sense with respect to maximum inclination line on the tangent plane at each tool contact point. One surface can be ma-

Fig. 4. HHP test part

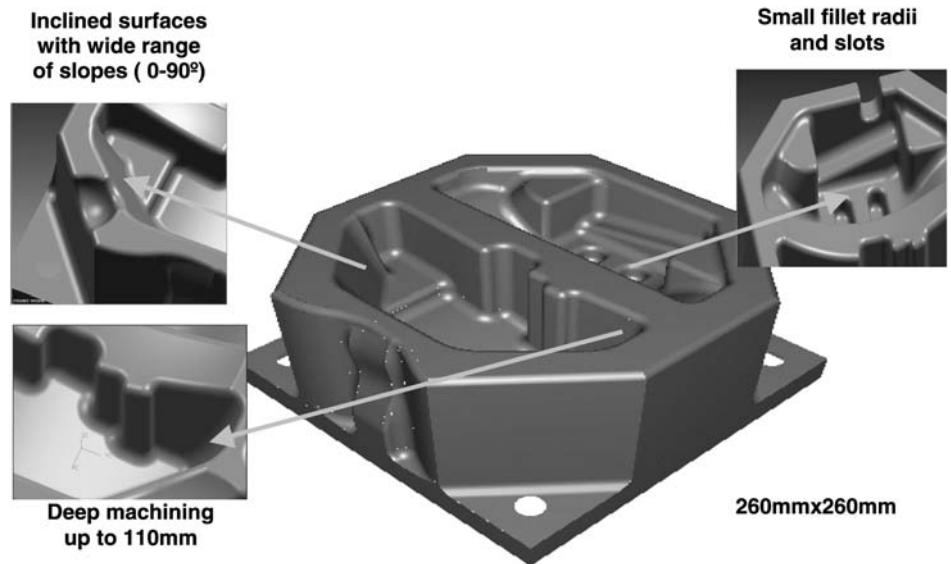
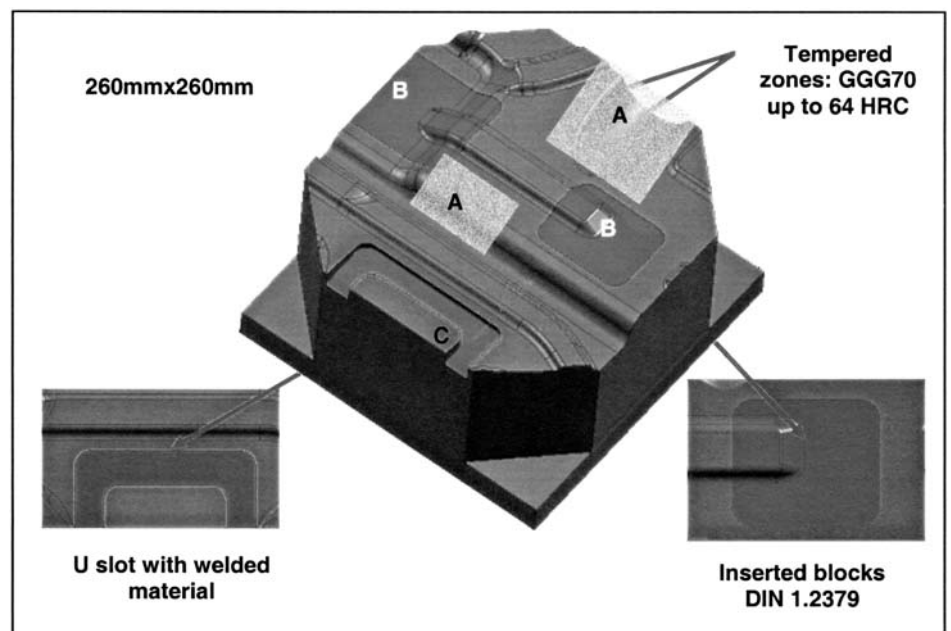


Fig. 5. VHSP test part



chined to meet the requirements of precision and roughness with some selected values for these angles, and on the contrary, with other orientations deriving from them.

2.3 Variable hardness surface part (VHSP)

This part is a smooth surface with a shape typical of large punches and dies. Its main feature is the presence of three different materials/hardness zones. Thus, the block part and most of its surface is constituted of a globular iron casting GGG70 (ASTM 100-70-03) with a hardness 280 HBN. Parts marked “A” in Fig. 5 are tempered from the GGG70 by an induction surface treatment. Its mean hardness is around 60 HRC. The two blocks marked “B” are made of DIN 1.2379 (AISI type D3) steel tempered at 64 HRC. The area marked “C” is a U-slot where Stellite Alloy 1 (53 HRC) material has been deposited.

3 Precision in machining

In general, there are several factors in machining that result in a lack of precision in final parts. Factors include those resulting from the CAM stage, which are caused by the approximation of the tool paths produced by current commercial software on the desired surface; and those resulting from insufficient resolution of the CNC control loops corresponding to the choice of both feed forward and look-ahead parameters. There are also errors due to the construction and stiffness of the actual machine tools, which are directly related to vibration in machining, inertial tool-path inaccuracy and thermal distortions. Various problems may also arise from the tool clamping systems, or from thermal deflection of the workpiece and tools. Error can be defined as any deviation in the actual position of the mill cutting edge from the position that was theoretically programmed to produce a part within a desired tolerance.

In the time-consuming process of HSM machining of large dies, there are three important aspects affecting the accuracy of the surfaces. First, tool runout [18, 19] causes a non-uniform cutting of the tool edges and leads to the uneven wearing of milling tools and wave marks on the final surface. As shown in Fig. 6, runout can be adjusted under a threshold value using a pre-setting station. Common values are between 3–10 μm , depending on the type of toolholder (i.e., less than 4 μm for thermal shrinkage, and around 8 μm for collet clamped ones), and the skill of workers is usually high in stamping firms. These workers usually take control of the expensive machines, are able to use the CAM stations set next to the HSM machines (known as work-on-plant stations), and can use the stations for tool pre-settings.

Second, tool wear can be systematically checked during the machining process with regular measurement procedures (even in the same machine if it has a laser pre-setting device), as shown in Fig. 6. The wear parameter of flank milling should be kept under 0.2–0.3 mm, although higher values are allowed if the cutting noise is low.

Third, there are important errors associated with the deflection of cutting tools (or distortion of the entire machine under the action of the cutting force). In tests performed by the authors on hardened steel (52 HRC) [20], error derived from tool deflection in ball-end finishing processes exceeded 40 μm ; and in other research, error of more than 100 μm were collected in [21]. In the end milling of wrought aluminium alloy with a 6 \emptyset mm tool, error as high as 170 μm are described in [22] when an axial depth of cut of 10 mm is used. In complex surface manufacturing, tolerances for dimension are commonly within the range of 0.05–0.1 mm for stamping dies and less than 0.04 mm for injection moulds.

The higher the material hardness, the higher the cutting forces. Therefore, errors due to the tool deflection are also larger. In dies for AHSS, inclined surfaces tend to be even harder than those of steels used in injection moulds. To control de-

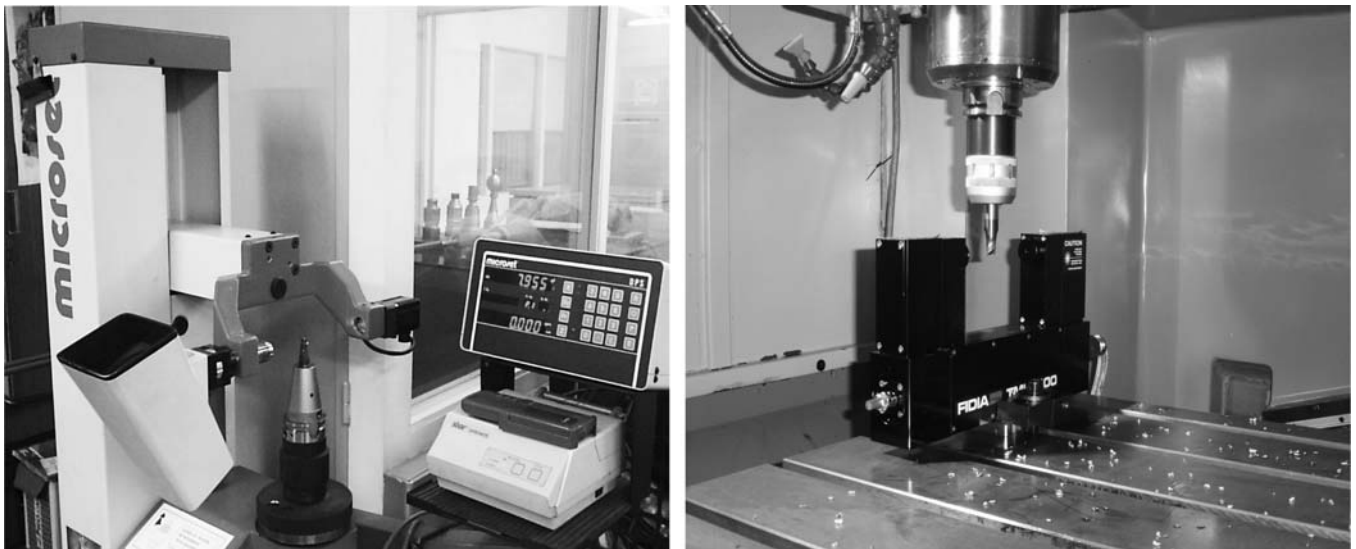


Fig. 6. Left – tool pre-setting machine; right – tool measurement system (TMS)

flexion error, two factors must be studied: the stiffness of the machine-spindle-shank-tool system, and the estimation of the cutting forces using a mechanistic model.

3.1 Stiffness of the machine tool system

We also studied the flexibility of the chain formed by the machine-spindle-shank-tool. This implies the entire machine tool, including the spindle, the shank interface with the spindle, the interface between tool and toolholder, and the tool itself. Table 1 provides a brief outline of the results and the calculation methods used. The details of this investigation are complex and beyond of scope of this paper. However, in Fig. 7 some aspects are shown:

- Left – displacement sensors have been used for the calculation of both angular and radial displacement stiffness coefficients.
- Centre – the stiffness chain involved some links; each one has been described for stiffness considerations.

- Right – the entire system (except for the tool) is characterised by two equivalent stiffness coefficients. In the figure, values for three different tools are shown. The clamping stiffness of the tool in the collet depends on tool diameter; the clamping stiffness decreases with the diameter of the tool. Consequently, tools with smaller diameters are more flexible not only due to their diameter, but also due to their lesser grade of clamping.

The system to be studied is a cantilever beam with a clamping modelled by K_δ and K_θ . Cutting forces are applied to it to estimate the deflection error. With a simple FEM model, the deflection of the tool tip related to a force can be calculated.

To obtain a good estimation of the deflection on the floor, a useful diagram has been proposed and is shown in Fig. 8. Here, the deflection coefficients with respect to the slenderness of the tool (factor L^3/D^4) are presented. This tool factor is more significant than the simpler L/D (where L is the length of the tool overhang out of the toolholder and D the tool diameter) because

Table 1. Influence of tilt and feed angles on cutting forces, deflection and error

| Chain link | Measurement method of stiffness | Characteristic stiffness coefficient | Usual values |
|-------------------------|---|--|---|
| Machine Tool stiffness | (a) FEM simulation during the design of machine | K_x (N/ μ m) K_y (N/ μ m) K_z (N/ μ m) | 20–62 30–60 60–100 |
| | (b) Experimental test on machine | | (values for gantry type machines) |
| Shank-spindle interface | Experimental test using non-contact inductive sensors in two points: one in spindle and other in shank | K_θ (N.m/ μ m) K_δ (N/ μ m) | 7000–10 000 80–100 (values for HSK 63) |
| Interface collet-tool | Experimental test using non-contact inductive sensors in two points: one in toolholder and other in tool body | K_θ (N.m/ μ m) K_δ (N/ μ m) | 200–800 80–100 (values for collet-nut type toolholders) |
| Tool | (a) FEM method | K_δ (N/ μ m) | 0.15 for 6 ϕ mm (overhang 66 mm) |
| | (b) Analytical models | | 4.4 for 12 ϕ mm (overhang 55 mm) |
| | (c) Experimental tests | | 1.6 for 16 ϕ mm (overhang 112 mm) (values for hard metal tools) |

Fig. 7. Simplified calculation of the system stiffness. Left – measurement of displacement at several points; centre – model of the system; right – equivalent system

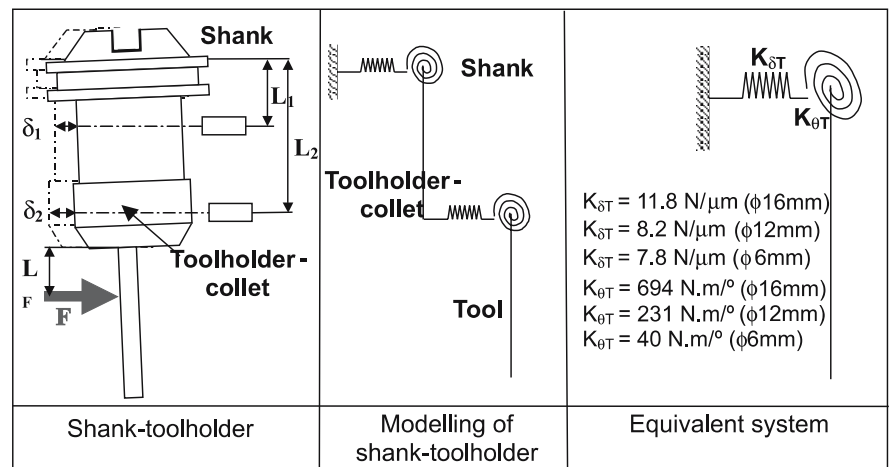
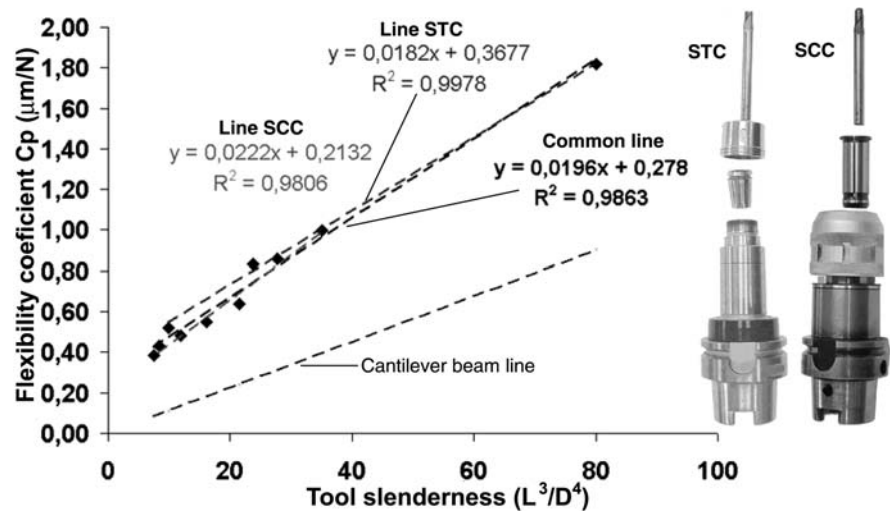


Fig. 8. Approximate extrapolation lines of flexibility coefficients: lines for shank with cylindrical collet (SCC) and shank with tapered collet (STC), where the line common to all cases is the line of cantilever beam



the basic formulation for a cantilever beam is directly related to the tool geometry through it. This can be described by the following:

$$\delta = \frac{64 F L^3}{3\pi E D^4} \quad (1)$$

There are four curves, two relating to the type of shank used – a shank with a tapered or cylindrical collet – and a line common to both types. This line corresponds to the cantilever beam with perfect clamping. The user obtains the value of factor L^3/D^4 for the given case to find the value of the deflection coefficient C in the graph using any of the three proposed curves – shank with cylindrical collet (SCC), shank with tapered collet (STC) or common line. The cutting forces obtained by an empirical method (mechanistic), multiplied by this factor C_P (or $1/K_P$), allow for the deviation from the central point of the tool to be obtained, and therefore the error due to the deflection of the tool. So deflection at the tool tip can be calculated by a basic relationship:

$$\delta = C_P * F \quad (2)$$

where F is the force applied perpendicular to the tool-axis. The proposed method would only be valid in cases similar to those studied, that is to say with shanks with a similar stiffness and machine-tools with similar characteristics. But even so, it could be used as a system to obtain a value that is closer to the real value than the cantilever beam model. The line corresponding to the perfectly clamped cantilever beam is also presented in Fig. 8, and the divergence between this line and the real one can be deduced. The difference between this case and the real case can be observed in this way. It can also be used to approximate the proportion between the corresponding deflection of the tool and that corresponding to the rest of the system.

3.2 Prediction of the cutting forces

Recently, different cutting forces models for ball-end milling have been presented [23–25]. These models are based upon

a semi-mechanistic approach, so they estimate cutting forces by dividing the cutting edge into small elements and applying to each of these a simple mathematical model that calculates the cutting force based on the un-deformed chip thickness and several cutting coefficients. These coefficients depend on the part material, as well as the tool material and geometry. Finally, the total cutting force is calculated by adding the effort of each discrete cutting edge. The main advantage the semi-mechanistic models as compared to the numeric models is the speed calculation; but on the other hand, the main disadvantage is the need to calculate the empirical coefficients of the model. Semi-mechanistic models use coefficients that depend on the part material, the material and coating of the tool, and the geometry of the cutting edges. Thus, it is not possible to create a unique database of coefficients; this requires calculating them for each couple tool/material by experimental tests. In the case of die materials for AHSS forming tools (and the most spread tools for this application) – type K10 with TiAlN-coating – we studied two materials and five or six types of tools. As such, a short characterization of coefficients was done.

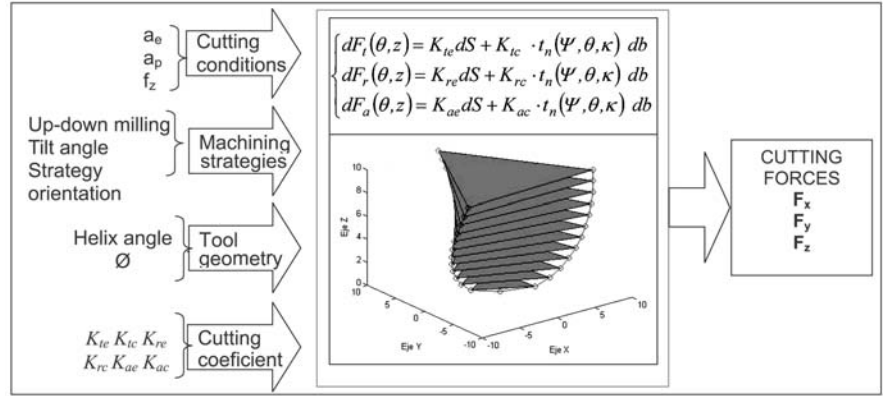
In past research [25], we have developed a model which calculates the forces for ball-end milling tools working on inclined planes from 0° to 90° . This feature is very useful for the milling of moulds and dies where surfaces are of sculptured or freeform type. The model has been programmed in C language, and is able to obtain the three components of the cutting forces in milliseconds. In Fig. 9, the input and output of the force calculation is shown. This module can be used by CAM operators for both three-axes and five-axes machining.

3.2.1 Possibilities in three-axes machining

Three-axes machining is a common practice in the manufacturing of large dies, where it is used for freeform and large surfaces, such as automotive body parts. In this case, there are two ways to calculate the cutting forces:

1. The model can be used a posteriori. In this case, the objective is the validation of a previously programmed tool path.

Fig. 9. Input and output for force calculation (model described in [25])



A maximum admissible value for the cutting force is set, and the programmed tool path is accepted if force is kept below this maximum value. This estimation is performed in critical areas like the die and punch interfaces, contact areas, etc.

- The model can be used to evaluate a priori the performance of different machining strategies at some user-defined control points on the surface. The optimum tool path will be the one that minimizes the value of the cutting force on those points. This option allows a “scientific” selection of the best machining strategy, as is shown in the machining of the CSP (Sect. 4). The optimum toolpath reduces the maximum force perpendicular to the tool axis, and the higher this force, the larger the tool deflection. The relationship between force and surface error is geometrically defined in Fig. 10, resulting in:

$$\varepsilon = \delta \sin \alpha . \tag{3}$$

Figure 11 shows the methodology for the implementation of the a priori option, in the case of the CSP part. The user, by projecting a grid on the surface (left), defines a number of control points on the surface. The excess of material that must be machined at each point is calculated, and then the model for the prediction of the cutting forces is applied. Results are obtained in 15° increments (24 directions from each control point) for both downmilling (climb milling) and upmilling (conventional milling), as shown in the centre of the diagram. Once the results are obtained, the best machining strategy is established (right).

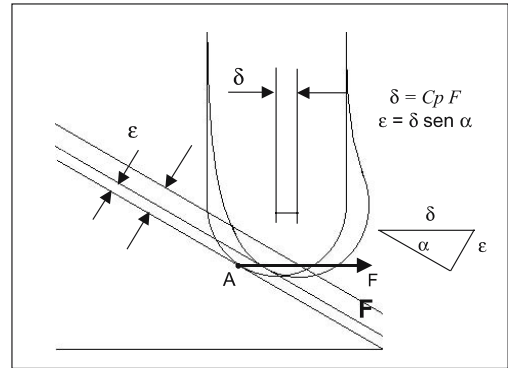


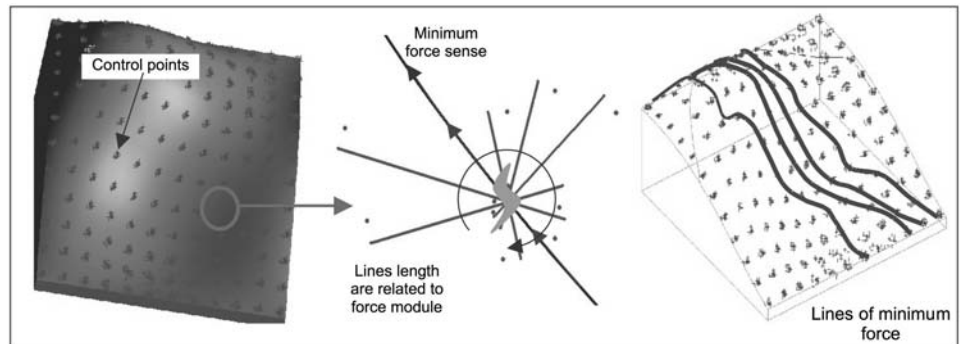
Fig. 10. Relationship between tool deflection δ and dimensional error ε

This method can be applied in the case of sculptured surfaces and/or free surfaces. In very sharp geometries, or those with very little curvature, there are other considerations to be taken into account, such as avoiding unexpected material stocks due to previous operations, or the rational succession of milling operations. In the case of this methodology, a case of the latter for pocket milling is rare.

3.2.2 Possibilities in five-axes machining

In the case of five-axes machining, an on-line utility has been developed in order to assess the best orientation of the tool on each

Fig. 11. On-line application of the feed sense selection in the case of the CSP part: left – definition of control points; centre – calculation in each 15° (down-milling); right – selection of tool paths



surface before calculating the toolpath. Users, in this case the CAM operator, can freely select both the tool tilt angle and the feed direction on the surface. With this utility, operators can evaluate multiple possibilities that minimise both the cutting forces and the length of tool simultaneously.

Cutting forces can change significantly with a variation of tilt and sense angles. Table 2 shows the value of cutting force components are projected perpendicularly to the tool axis (in the plane which contains the maximum slope line to surface). It also shows tool deflection by applying the flexibility coefficient from

Fig. 8, $C_p:1.3 (L^3/D^4 : 55)$, and Eq. 2, and results in the projection of deflection perpendicular to the tangent plane at one surface point, as described by Eq. 3. This projection is directly related to dimensional error. Here, we have found that:

- When tilt angle is zero, the projection of deflection perpendicular to surface is always zero, even if tool deflection is high (for tilt and feed angles $0^\circ, 240^\circ$ in upmilling this is $70 \mu\text{m}$, and $0^\circ, 0^\circ$ in downmilling this is $68 \mu\text{m}$). This case seems to be the best for precision, but there remains cutting

Table 2. Value of force for different tilt and feed angles (the reference for feed sense is indicated)


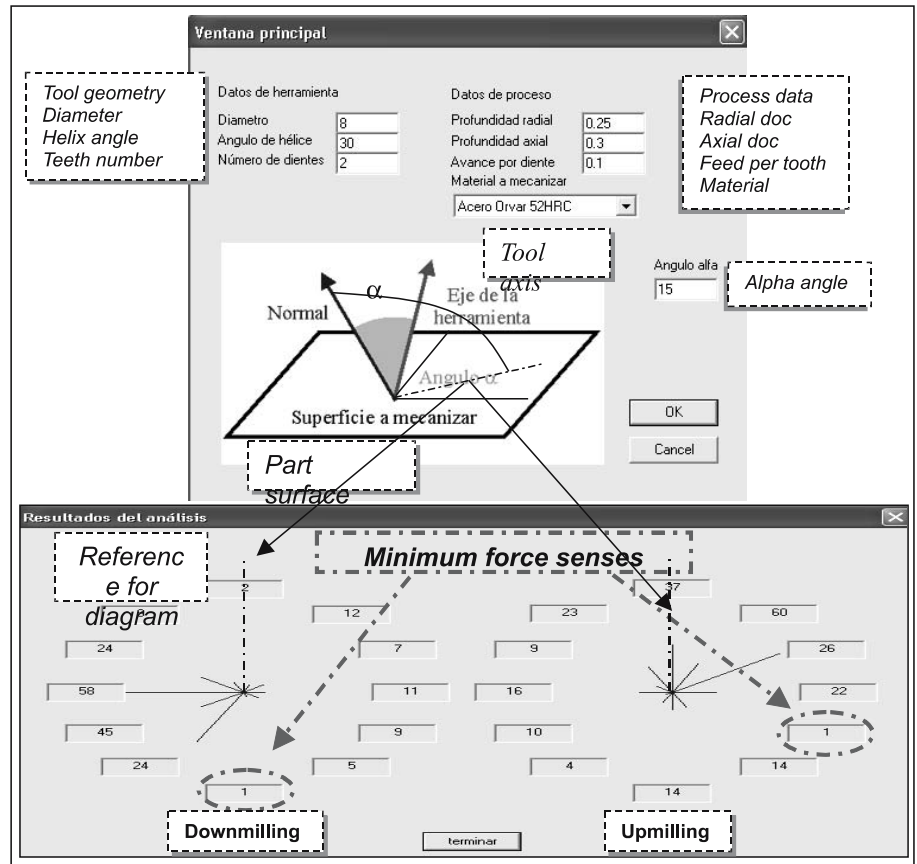
| Tilt | Case  | Force deflection (N) | UP-MILLING | | DOWN-MILLING | | | |
|------|---|----------------------|---------------------------------|------------------------------------|--------------------|------------------------|-------------------------|------|
| | | | Tool expected (μm) | Error deflection (μm) | Force expected (N) | Tool (μm) | Error (μm) | |
| 0° | 0° | 25 | 33 | 0 | 51 | 68 | 0 | |
| | 30° | 6 | 8 | 0 | 35 | 46 | 0 | |
| | 60° | 28 | 37 | 0 | 8 | 11 | 0 | |
| | 90° | 47 | 62 | 0 | 19 | 25 | 0 | |
| | 120° | 29 | 39 | 0 | 7 | 9 | 0 | |
| | 150° | 7 | 9 | 0 | 32 | 42.5 | 0 | |
| | 180° | 25 | 33 | 0 | 47 | 62.5 | 0 | |
| | 210° | 45 | 60 | 0 | 50 | 66.5 | 0 | |
| | 240° | 53 | 70 | 0 | 41 | 54.5 | 0 | |
| | 270° | 47 | 62 | 0 | 19 | 25 | 0 | |
| | 300° | 29 | 38 | 0 | 9 | 12 | 0 | |
| | 330° | 7 | 9 | 0 | 34 | 45 | 0 | |
| | 15° | 0° | 2 | 3 | 0.6 | 36 | 48 | 12.5 |
| | | 30° | 11 | 15 | 4 | 42 | 56 | 14.5 |
| 60° | | 16 | 21 | 5.5 | 14 | 19 | 5 | |
| 90° | | 21 | 28 | 7 | 18 | 24 | 6 | |
| 120° | | 8 | 11 | 2.5 | 4 | 5 | 1 | |
| 150° | | 3 | 4 | 1 | 11 | 15 | 4 | |
| 180° | | 8 | 10 | 3 | 16 | 21 | 5.5 | |
| 210° | | 23 | 31 | 8 | 15 | 20 | 5 | |
| 240° | | 34 | 45 | 11.5 | 17 | 23 | 6 | |
| 270° | | 42 | 56 | 14.5 | 4 | 5 | 1 | |
| 300° | | 22 | 30 | 7.5 | 14 | 19 | 5 | |
| 330° | | 7 | 9 | 2.5 | 24 | 32 | 8 | |
| 30° | | 0° | 1 | 1 | 0.5 | 29 | 39 | 20 |
| | | 30° | 7 | 9 | 4.5 | 48 | 64 | 32 |
| | 60° | 4 | 5 | 2.5 | 23 | 31 | 15 | |
| | 90° | 9 | 12 | 6 | 12 | 16 | 8 | |
| | 120° | 4 | 5 | 2.5 | 1 | 1 | 0.5 | |
| | 150° | 4 | 5 | 2.5 | 10 | 13 | 6.5 | |
| | 180° | 1 | 1 | 0.5 | 8 | 11 | 5 | |
| | 210° | 19 | 25 | 12.5 | 1 | 1 | 0.5 | |
| | 240° | 33 | 44 | 22 | 6 | 8 | 4 | |
| | 270° | 39 | 52 | 26 | 11 | 14.5 | 7.5 | |
| | 300° | 11 | 15 | 7 | 6 | 8 | 4 | |
| | 330° | 3 | 4 | 2 | 17 | 23 | 12 | |
| | 45° | 0° | 1 | 1 | 1 | 25 | 33 | 24 |
| | | 30° | 3 | 4 | 3 | 53 | 70.5 | 50 |
| 60° | | 2 | 3 | 2 | 31 | 42 | 29 | |
| 90° | | 14 | 18 | 13 | 7 | 9 | 7 | |
| 120° | | 4 | 5 | 4 | 3 | 4 | 3 | |
| 150° | | 3 | 4 | 3 | 5 | 7 | 4.5 | |
| 180° | | 1 | 1 | 1 | 1 | 2 | 1 | |
| 210° | | 18 | 24 | 17 | 1 | 2 | 1 | |
| 240° | | 32 | 43 | 30 | 11 | 14 | 10 | |
| 270° | | 21 | 28 | 20 | 12 | 16 | 11 | |
| 300° | | 4 | 5 | 4 | 3 | 4 | 3 | |
| 330° | | 2 | 2 | 2 | 15 | 20 | 14 | |

Fig. 12. Top – interface of the analysis utility for the selection of the correct tool orientation (translation to English from Spanish in insets); bottom – result maps



at the tool tip where cutting speed is zero. This fact usually causes tool breakage, so this case is avoided when possible.

- When tilt angle is 15° , good senses are 0° in upmilling and 270° in downmilling. But if tilt angle is 30° , a better feed sense is 210° in downmilling.
- When tilt angle is 45° , errors are larger – up to $30\ \mu\text{m}$ for 240° -upmilling and $50\ \mu\text{m}$ in 30° -downmilling.

Based on the calculation of cutting forces, a multi-stage procedure was developed for optimal programming:

1. Separation of surface areas taking into account several criteria:
 - Division of a part in similar zones with the same surface and precision requirements, which implies only smooth changes in tool orientation and considers several faces as one case of machining. In many body parts (and their corresponding dies), large surfaces can be formed by summing up the adjacent small areas. This makes the preparation of CNC programs much easier.
 - The tool used for part faces is also used to determine similar requirements of roughness. This reduces the number of tool changes, with a rationalization of tool path.
2. Selection of the orientation angle between the tool axis and the surface, which is measured between the tool axis and the perpendicular to the surface, is called tilt angle α . This angle is restricted by the tool overhang with respect to the

depth of the parts to be machined, and as such avoids tool interferences with inclined walls. The deeper the part to be machined, the narrower the taper angle in which the tool axis can be oriented. One of the tool axes is selected (all the following steps reach similar results) depending on the access of tool to part.

3. Selection of the feed sense with respect to the intersection of the tangent plane and the plane containing both the tool axis and the vector perpendicular to tangent plane. This angle is ϱ , and it ranges from 0° to 360° in both downmilling and upmilling.

In Fig. 12, the aspect of the user interface (translated from Spanish to English) is shown, as well as a circular diagram result for the downmilling and upmilling cases, where tool rotation is always in a clockwise direction. The larger the line, the higher the cutting force. So in this case (Fig. 12), for example, the minimum force is achieved by machining at a -180° (downward) for downmilling, and at a -120° (downward) for upmilling.

4 Results of test part machining

The aforementioned machining procedures have been applied to the CSP, HHP and VHTP test parts. Results are detailed in the following subsections.

4.1 Machining of the CSP test part

The freeform CSP test part features smooth surfaces and was machined in three feed senses, given different precision maps, as shown in Table 3. Here, the milling strategy, the cutting force perpendicular to tool axis, and the surface measurement in a coordinate measurement machine (CMM) are presented for the three cases. Measurements in CMM require a good alignment of the part in the CMM marble, so several reference planes were also machined in the part.

The first two tests were performed using the zig-zag strategy. In zig-zag, one pass is in downmilling conditions, and the

return pass is in upmilling, so dimensional errors are difficult to predict with a formulation like Eq. 1 and Eq. 2. But usually, dimensional errors are a balance of those corresponding to each of the cases. In past research [20, 26] considering the results of different machining strategies (upmilling-downmilling, upward-downward) on different planes, very different errors were measured for the downmilling and upmilling cases under the same cutting conditions of feed, depth of cut and cutting speed. If high precision is expected, this is not the optimum tool path, but die manufacturers prefer it because there are no idle times. Therefore, since this cutting strategy will be followed in practice, dimensional errors are admissible. The CSP

Table 3. Cutting forces and measurements by a coordinate measurement machine for the CSP part

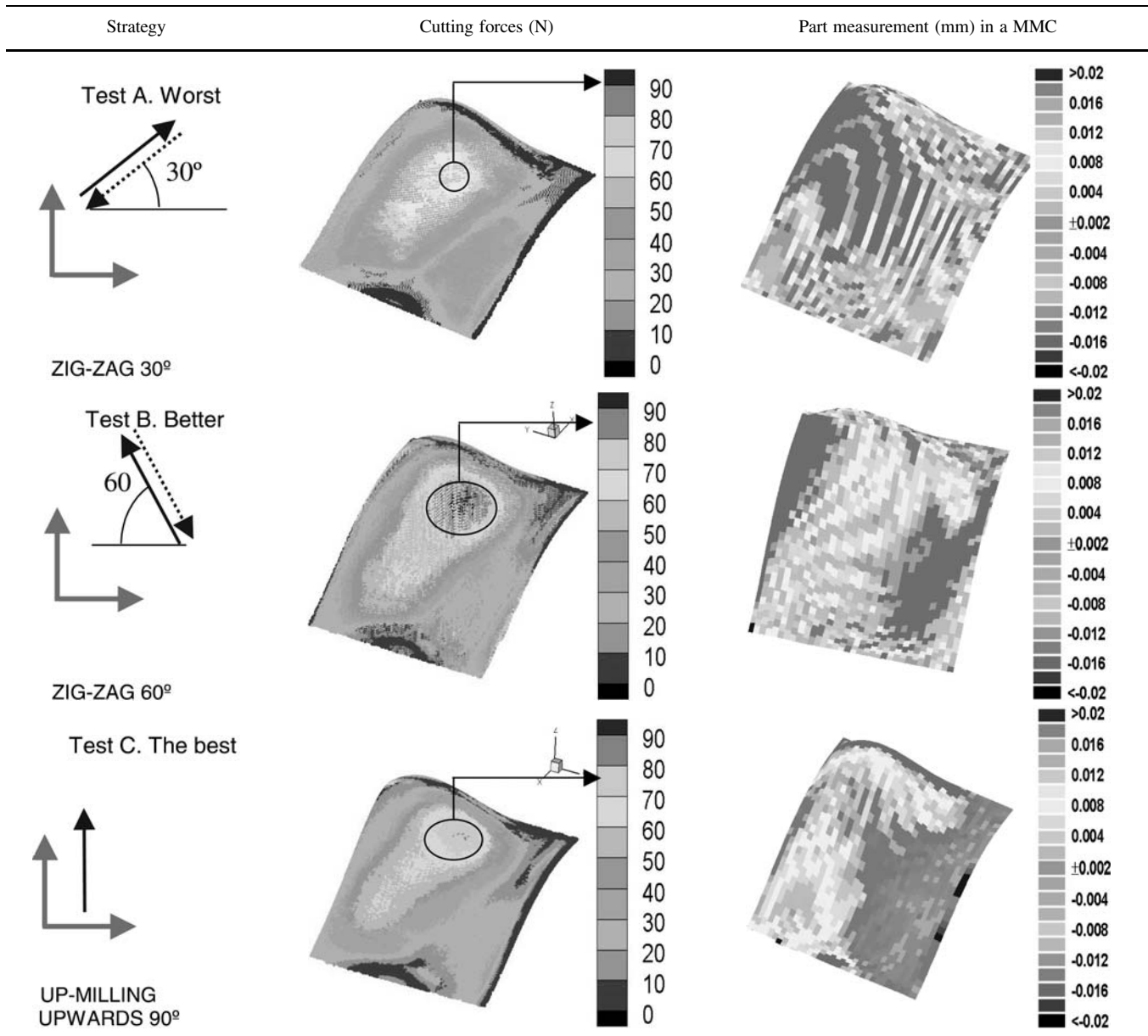
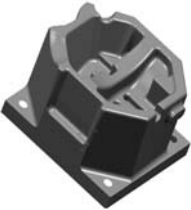
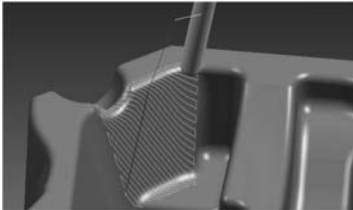

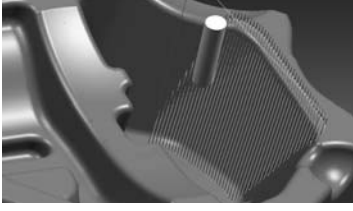

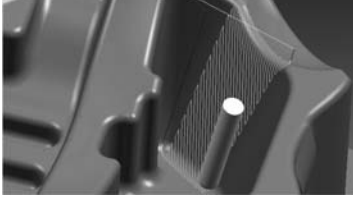

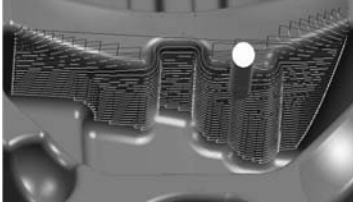



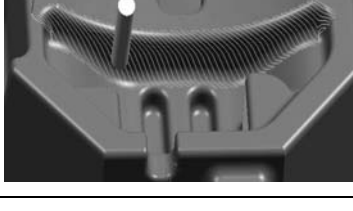



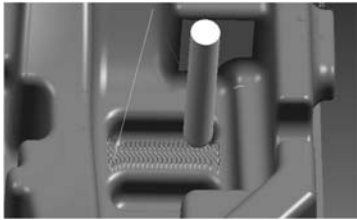

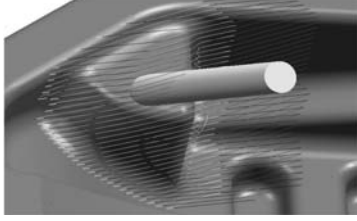

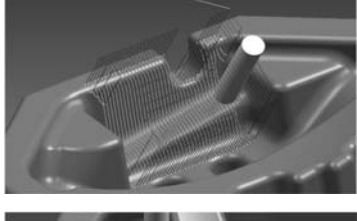

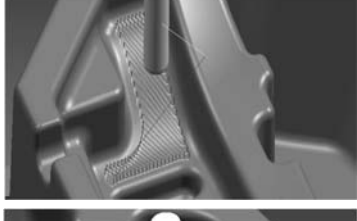

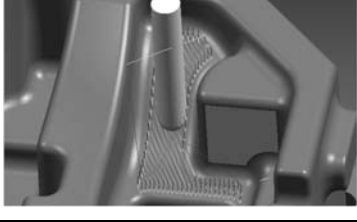
Table 4. Selection of proper cutting types for the HHP(I)

| | Selected zone | Detail of toolpath | Cutting conditions | Strategy and dimensional error |
|---|---|---|--|---|
| A |  |  | $F = 700$ m/min $N = 4100$ rpm $a_p = 0.3$ mm $a_e = 0.27$ mm Ball-end mill $\varnothing 12$ Overhang: 50 mm | Zig-Zag cutting Feed sense: 30° Toll tilt angle: 15° Dimensional error 12 μ m |
| B |  |  | $F = 700$ m/min $N = 4100$ rpm $a_p = 0.3$ mm $a_e = 0.27$ mm Ball-end mill $\varnothing 12$ Overhang: 50 mm | Zig cutting, downmilling Feed sense: 15° Toll tilt angle: 15° Dimensional error 5 μ m |
| C |  |  | $F = 700$ m/min $N = 4100$ rpm $a_p = 0.3$ mm $a_e = 0.27$ mm Ball-end mill $\varnothing 12$ Overhang: 50 mm | Zig-Zag cutting Feed sense: 45° Toll tilt angle: 15° Dimensional error 42 μ m |
| D |  |  | $F = 700$ m/min $N = 4100$ rpm $a_p = 0.3$ mm $a_e = 0.27$ mm Ball-end mill $\varnothing 12$ Overhang: 55 mm | Zig-Zag cutting Feed sense: 90° Toll tilt angle: 23° Dimensional error 30 μ m |
| E |  |  | $F = 700$ m/min $N = 4100$ rpm $a_p = 0.3$ mm $a_e = 0.27$ mm Ball-end mill $\varnothing 12$ Overhang: 55 mm | Zig cutting, downmilling Feed sense: 45° Toll tilt angle: 10° Dimensional error 2 μ m |
| F |  |  | $F = 700$ m/min $N = 4100$ rpm $a_p = 0.3$ mm $a_e = 0.27$ mm Ball-end mill $\varnothing 12$ Overhang: 50 mm | Zig-Zag cutting Feed sense: 57° Toll tilt angle: 30° Dimensional error 40 μ m |

part demonstrates the features of very large parts such as bonnets, lateral sides, ceilings and wings, where machining times more than 40 h. The use of only zig toolpaths, which bring

the tool back to the starting point in each passing path in G00 maximum linear feed, increases the machining time by approximately 20%–30%.

Table 5. Selection of proper cutting types for the HHP(II)

| | Selected zone | Detail of toolpath | Cutting conditions | Strategy and dimensional error |
|---|---|---|--|--|
| A |  |  | $F = 600$ m/min $N = 3600$ rpm $a_p = 0.3$ mm $a_e = 0.3$ mm Ball-end mill $\varnothing 14$ Overhang: 50 mm | Zig cutting, downmilling Feed sense: 30° Toll tilt angle: vertical Dimensional error $0 \mu\text{m}$ |
| B |  |  | $F = 700$ m/min $N = 4100$ rpm $a_p = 0.3$ mm $a_e = 0.27$ mm Ball-end mill $\varnothing 12$ Overhang: 50 mm | Zig cutting, upmilling Feed sense: 30° Toll tilt angle: 60° Dimensional error $0 \mu\text{m}$, except in the marked zone where it is $38 \mu\text{m}$ |
| C |  |  | $F = 700$ m/min $N = 4100$ rpm $a_p = 0.3$ mm $a_e = 0.27$ mm Ball-end mill $\varnothing 12$ Overhang: 50 mm | Zig cutting, downmilling Feed sense: 90° Toll tilt angle: 45° Dimensional error $14 \mu\text{m}$ |
| D |  |  | $F = 600$ m/min $N = 3600$ rpm $a_p = 0.3$ mm $a_e = 0.3$ mm Ball-end mill $\varnothing 14$ Overhang: 50 mm | Zig cutting, downmilling Feed sense: 30° Toll tilt angle: 0° Dimensional error $0 \mu\text{m}$ |
| E |  |  | $F = 600$ m/min $N = 3600$ rpm $a_p = 0.3$ mm $a_e = 0.3$ mm Ball-end mill $\varnothing 14$ Overhang: 50 mm | Zig cutting, downmilling Feed sense: 30° Toll tilt angle: 0° Dimensional error $9 \mu\text{m}$ |

In test A, the worst results are obtained using the zig-zag procedure, with errors greater than $20 \mu\text{m}$ at some points. At the same time, cutting forces were recorded and mapped in a colour diagram. As shown, only a small area was machined with forces near 90 N. When tool deflection occurs at the point where it attacks the surface in tangential tool paths, error results from the following: (a) forces are higher, and their component is perpendicular to and contained within the plane formed by the tool axis; and (b) the maximum slope line is the higher.

Case B shows better results, with a smaller area with errors of greater than $20 \mu\text{m}$. Similarly to previous case, errors are located in zones where the force component perpendicular to the tool axis is high.

In test C, the best results were obtained. Here, only one sense of machining in up-milling conditions was used. The good precision in this case, only achieved in the downmilling type of cutting, is due to the relatively small force component.

From these results, die manufacturers have decided to use case B, since its milling time is not too long and its precision is adequate.

4.2 Machining of the HHP test part

This part demonstrates several features of the tempered insert blocks of both punches and dies. The hardness of this material is greater than that of mould steels. Success in machining has been

| $\varnothing 12\text{mm}$ $a_p 0,2\text{mm}$ $a_e 0,2\text{mm}$ | f_z mm/edge | V_c m/min | F (m/min) | S (rpm) |
|---|------------------|----------------|----------------|--------------|
| Free Surface | 0,077 | 905 | 3697 | 24000 |
| Tempered Zone A | 0,07 | 357 | 1326 | 9470 |
| Insert blocks Zone B | 0.061 | 236 | 764 | 6260 |
| Welded Zone C | 0.077 | 583 | 2395 | 15462 |




Fig. 13. Machined VHTP test part, indicating the cutting conditions for zones

achieved by using the right selection of tool tilt and feed sense. Finishing takes more than 20 h in a five-axes machine, and makes use of the orientation possibility for the tool with respect to the surface of the part. CAM work in this case was 40 h long.

Results are presented in Tables 4 and 5, where the tool, cutting conditions, strategy, tilt and feed sense angle are detailed. The measured error of surface with respect to the theoretical value is indicated as well. This error has been measured with a contact probe, (Renishaw), and represents the difference at a point after one finishing pass and a contiguous one taken at a small square that was machined twice. In this way, the second pass eliminates the stock allowance left by tool deflection in the first cutting pass. With this relative measurement, the effect of workpiece misalignment on the CMM is reduced. However, this error is always present, even if an alignment procedure based on three reference planes on the original workpiece is carried out. This procedure was preliminary used, but the lack of precision of the workpiece setup in both the machine tool and the CMM made it impossible to discern tool deflection from setup errors.

Results of tool deflection are within the requirements of the part. In the worst case, this was $42\ \mu\text{m}$ (Table 2 zone C), and occurred in a zone where the tilt angle was below 20° due its depth. This value is considered to be low enough, because the concerns of dimensional precision are not significant. High precision is achieved in the smooth area (Table 3 zone D) where tilt angle is 0° and feed sense 30° ; therefore, in this area, machining is like a three-axes operation.

After the machining of this complex part, and taking into account the good precision achieved by the estimation of the correct tilt and feed angles through force estimation, the utility has been implemented in the die company as a toolbox on-line utility running simultaneously with the CAM system.

4.3 Machining of the VHTP test part

In Fig. 13, a picture of this part after machining is shown. Breakage or chipping of tool teeth did not occur, and finishing all surfaces was conducted with only one $\varnothing 12\ \text{mm}$ ball-end milling

tool, hard metal submicron grade (type K10) coated with TiAlN monolayer. This is a commonly used tool in moulding and die manufacturing. Four areas were previously defined, with the programmed feed and cutting speed recommended by the tool supplier. The values are presented in Fig. 13. All machining was done in zig-zag, which is preferred in large die manufacturing. In the zone of material deposition, where Stellite was deposited over one U-slot, a flattening program was first performed. This short program does not increase production time, and is absolutely necessary to ensure tool durability. An adequately smooth acceleration of spindle and machine axes due to continuous change in F (linear feed) and S (rotational speed) are provided by motor drive control.

After this test, a nearby manufacturing company is applying this approach and achieving good results and process performance.

5 Conclusions

There are two main problems to be solved in the high-speed finishing of forming tools for the processing of advanced high-strength steels. The first problem is the unacceptable dimensional error resulting from tool deflection due to cutting forces; and the second is the simultaneous finishing of surfaces with different hardness in the same operation and with the same CNC program.

The first problem is solved during the definition of CNC programs in the CAM production stage, through estimation of the cutting forces. Three working types are evaluated depending on whether it is a three-axes case or if five-axes machining is possible. In the latter, a utility for the proper selection of tilt and feed sense angles based on the minimization of cutting forces was developed. Two test parts have been machined, and results show that this is the key to maintain adequate precision for die manufacturing.

In the case of the second problem, the surface is divided into zones, and the linear feed and cutting speed is determined based on hardness level. These values are then applied by CAM

operator. A postprocessor utility inputs the values of feed and spindle rotation into the CNC program (usually a zig-zag tool path obtained by CAM) when a transition between two areas is detected.

Our approach has been used by die manufacturers, demonstrating that firms with an adequate, user-friendly interface can make technological advances in process modelling. Industrial profit is achieved with a better CAM procedure and new software tools.

References

1. Integrated Manufacturing Initiative Inc. (2000) Integrated manufacturing technology roadmapping project. Integrated Manufacturing Initiative, Oak Ridge, TN
2. Institute for Prospective Technological Studies (2003) FUTMAN: Future of manufacturing in Europe 2015 – 2020 – the challenge for sustainable development, European Union report. European Commission, Joint Research Centre, Institute for Prospective Technological Studies, Seville
3. International Iron and Steel Institute (2004) AHSS guidelines. <http://www.worldautosteel.org/>
4. López de Lacalle LN, Lamikiz A, Sánchez JA, Arana, JL (2002) Improving the surface finish in the high-speed milling of stamping dies. *J Mater Process Technol* 123(2):292–302
5. Fallböhmer P, Rodríguez CA, Ozel T, Altan T (2000) High-speed machining of cast iron and alloy steels for die and mold manufacturing. *J Mater Process Technol* 121:104–115
6. Fallböhmer P (1998) Advanced cutting tools for the finishing of dies and molds. Springer-Verlag, Berlin Heidelberg New York
7. Lee SW, Yang DY (1998) An assessment of numerical parameters influencing springback in explicit finite element analysis of sheet metal forming process. *J Mater Process Technol* 80–81:60–67
8. Holmberg S, Enquist B, Thilderkvist P (2004) Evaluation of sheet metal formability by tensile tests. *J Mater Process Technol* 145(1):72–83
9. López de Lacalle LN, Lamikiz A, Sánchez JA, Salgado MA (2004) Cutting force integration at the CAM stage in the high-speed milling of complex surfaces. *Int J Comput Integr Manuf* (to be published)
10. Kang MC, Kim KK, Lee DW, Kim JS, Kim NK (2001) Characterization of inclined planes according to the variations of cutting direction in high-speed ball-end milling. *Int J Adv Manuf Technol* 17:323–329
11. López de Lacalle LN, Lamikiz A, Salgado MA, Herranz S, Rivero A (2002) Process planning for reliable high-speed machining of moulds. *Int J Prod Res* 40(12):2789–2809
12. Al-Fawzan MA, Al-Ahmari AMA (2004) Simultaneous determination of the optimal process mean and cutting speed for a manufacturing process. *Prod Plann Contr* 15(3):336–341
13. Schulz H (2000) *Hochgeschwindigkeits bearbeitung / High-speed machining*. Springer-Verlag, Berlin Heidelberg New York
14. Test part NCG 2004/T1 (2004) Test part HSC, NC Gesellschaft
15. Weinert K, Enselman A, Friedhoff J (1997), Milling simulation for process optimization in the field of die and mould manufacturing. *Ann CIRP* 46(1):30–34
16. Arnone M (1998) High performance machining. Hanser Gardner Publications, Ohio, USA
17. Duc E, Lartigue C, Thiebaut F (1998) A test part for the machining of freeform surfaces. In: *Proceedings of the Improving Machine Tool Performance Seminar*, San Sebastián, Spain, vol 1, pp 423–435
18. Aoyama T, Inasaki I (2001) Performances of HSK tool interfaces under high rotational speeds. *Ann CIRP* 50(1):281–284
19. Koshy P, Dewes RC, Aspinwall DK (2002) High-speed end milling of hardened AISI D2 tool steel. *J Mater Process Technol* 127:266–273
20. López de Lacalle LN, Lamikiz A, Sánchez JA, Salgado MA (2004) Effects of tool deflection in the high-speed milling of inclined surfaces. *Int J Adv Manuf Technol* 24:621–631
21. Kim GM, Kim BH, Chu CN (2003) Estimation of cutter deflection and form error in ball-end milling process. *Int J Mach Tool Manuf* 43:917–924
22. Choi K, Jerard RB (1998) *Sculptured surface machining: theory and applications*. Kluwer, Boston
23. Lee P, Altintas Y (1996) Prediction of ball-end milling forces from orthogonal cutting data. *Int J Mach Tool Manuf* 36(9):1059–1072
24. Bouzakis KD, Aichouh P, Efstathiou KD (2003) Determination of the chip geometry, cutting force and roughness in freeform surfaces finishing milling, with ball end tools. *Int J Mach Tool Manuf* 43:499–514
25. Lamikiz A, López de Lacalle LN, Salgado MA, Sánchez JA (2004) Cutting force estimation in sculptured surface machining. *Int J Mach Tool Manuf* 44(14):1511–1522
26. Kang MC, Kim KK, Lee DW, Kim JS, Kim NK (2001) Characterization of inclined planes according to the variations of cutting direction in high-speed ball-end milling. *Int J Adv Manuf Technol* 17:323–329